Nuclear Receptor Research
vol. 4 (2017), Article ID 101288, 17 pages
doi:10.11131/2017/101288

AgiAl Publishing House
http://www.agialpress.com/

Research Article

# Binding Site Analysis of the *Caenorhabditis elegans* NR4A Nuclear Receptor NHR-6 During Development

**Brandon Praslicka[1,4], Jeremy S. Harmson[1], Joohyun Kim[2], Vittobai Rashika Rangaraj[1], Aikseng Ooi[3], and Chris R. Gissendanner[1]**

[1] *Department of Basic Pharmaceutical Sciences, School of Pharmacy, and Biology Program, School of Science, University of Louisiana Monroe, Monroe, LA 71209, USA*
[2] *Center for Computation and Technology, Louisiana State University, Baton Rouge, LA 70803, USA*
[3] *Department of Pharmacology & Toxicology, College of Pharmacy, University of Arizona, Tucson, AZ 85721, USA*
[4] *Current Address: Department of Pharmacology & Toxicology, College of Pharmacy, University of Arizona, Tucson, AZ 85721, USA*

**Abstract.** Members of the NR4A subfamily of nuclear receptors make up a highly conserved, functionally diverse group of transcription factors implicated in a multitude of cellular processes such as proliferation, differentiation, apoptosis, metabolism and DNA repair. The gene *nhr-6,* which encodes the sole *C. elegans* NR4A nuclear receptor homolog, has a critical role in organogenesis and regulates the development of the spermatheca organ system. Our previous work revealed that *nhr-6* is required for spermatheca cell divisions in late L3 and early L4 and spermatheca cell differentiation during the mid L4 stage. Here, we utilized chromatin immunoprecipitation followed by next-generation sequencing (ChIP-seq) to identify NHR-6 binding sites during both the late L3/early L4 and mid L4 developmental stages. Our results revealed 30,745 enriched binding sites for NHR-6, ~70% of which were within 3 kb upstream of a gene transcription start site. Binding sites for a cohort of candidate target genes with probable functions in spermatheca organogenesis were validated through qPCR. Reproductive and spermatheca phenotypes were also evaluated for these genes following a loss-of-function RNAi screen which revealed several genes with critical functions during spermatheca organogenesis. Our results uncovered a complex nuclear receptor regulatory network whereby NHR-6 regulates multiple cellular processes during spermatheca organogenesis.

**Keywords:** *nhr-6,* NR4A, *Caenorhabditis elegans*, spermatheca, ChIP-seq.

**Corresponding Author**
Chris R. Gissendanner
gissendanner@ulm.edu

**Editor**
Evelyn Murphy

**Dates**
Received 11 April 2017
Accepted 09 July 2017





## 1. Introduction

Critical aspects of development rely on the proper spatial and temporal expression of genes necessary for a variety of cellular processes. Transcription factors (TFs) possess the ability to rapidly respond to various cell stimuli and regulate gene expression by binding to DNA sequences found in regulatory elements of a specific target gene. A complete understanding of genome-wide TF activities, including identifying both DNA binding regions and target genes, is key to understanding the often complex gene networks they regulate throughout the development of various tissue types. A widely used tool to investigate genome-wide DNA-protein

interactions *in vivo* is chromatin immunoprecipitation followed by next-generation sequencing (ChIP-seq). Both the ENCODE (Encyclopedia of DNA Elements) [1] and modENCODE (model organisms ENCODE) [2] projects have performed genome-wide ChIP-seq experiments on more than 140 TFs. However, little downstream analysis of target genes has been performed, particularly with respect to the role target genes play in the cellular processes known to be regulated by the TF being examined.

The NR4A subfamily of the nuclear receptor (NR) superfamily functions as TFs that act as early-immediate response genes which respond to a wide array of environmental stimuli and have been implicated in diverse physiological and cellular processes. [3]. Unlike ligand-dependent NRs, members of the NR4A subfamily are orphan receptors that are activated in a ligand-independent manner through posttranslational modifications [4]. Following activation, NR4A NRs bind as monomers or homodimers to the NGFI-B response element (NBRE) or Nur response element (NurRE) DNA sequences and both positively and negatively regulate target gene expression [5, 6]. The mammalian NR4A NR subgroup includes three closely related members-NR4A1 (Nur77), NR4A2 (Nurr1), and NR4A3 (NOR1)-that are highly expressed in energy-dependent tissues including skeletal muscle, heart, brain, and liver where they display tissue and cell-type specific functions. Due in part to their ability to rapidly regulate multiple target genes in response to cellular stimuli including growth factors [7], these receptors have been strongly implicated in developmental processes. Not surprisingly, several studies have confirmed important roles for NR4A NRs during the development of several cell types. Examples include T-cell, monocyte, myeloid and dopaminergic neuron differentiation [8–13], smooth muscle cell and hepatocyte proliferation [7, 14, 15], and mesenchymal stromal cell migration [16].

The sole *Caenorhabditis elegans* NR4A NR gene, *nhr-6* [17, 18], is a lineage-specific regulator of the spermatheca, a structurally simple but functionally complex reproductive organ that functions in oocyte fertilization and ovulation [19]. NHR-6 is robustly expressed in all developing spermathecal cells from the middle of the third larval stage (L3) into the middle of the fourth larval stage (L4), a key time point in spermatheca development. Previous work in our lab revealed that *nhr-6* has a dualistic function during spermatheca organogenesis, regulating both cell proliferation and differentiation [19, 20]. NHR-6 has also been shown to bind and activate transcription from the canonical NBRE site in mammalian HEK293 cells, while a cysteine to serine mutation in the DNA binding domain abolished its ability to bind DNA at the NBRE site [21], indicating biochemical conservation with mammalian NR4A NRs. The model organism *C. elegans* provides an excellent model with which to study genome-wide transcriptional networks during development. The lineage of each somatic cell is invariant and traceable, which provides a unique blueprint to map developmental regulatory networks [22]. Additionally, it possesses a compact genome that contains short intergenic regions which simplifies the process of assigning a TF binding site to a target gene [23].

Here, we have used ChIP-seq to examine NHR-6-DNA binding activities during spermatheca organogenesis. Following binding site identification in the ChIP-seq data set using a computational pipeline, further analysis was performed to validate binding sites, identify candidate target genes for each stage, and examine up-regulated signaling pathways. Utilizing a functionally biased approach to filter candidate target genes, we were also able to verify multiple target

genes with important roles in spermatheca development, indicating that they function within the NHR-6 regulatory network.

## 2. Materials and Methods

### 2.1. *C. elegans* strains

Strains were maintained and manipulated under standard conditions [24]. The following strains were obtained from the Caenorhabditis Genetics Center for use in this study: N2 (Bristol), GR1373 (*eri-1*(*mg366*)), and CZ411 (*vab-2*(*ju-1*)). DN73 (*jun-1*(*gk551*)) was previously generated in the Gissendanner lab [25], and the NHR-6::GFP transgenic line bearing an extrachromosomal array encoding a fully functional NHR-6::GFP, *sgEx15* [21], was chromosomally integrated and outcrossed to generate two independent integrated transgenic lines, *sgIs1* and *sgIs2* that rescued *nhr-6 (lg6001)* null mutants The resulting rescued integrated strains, *nhr-6 (lg6001); sgIs1* and *nhr-6 (lg6001); sgIs2* were closely examined and found to be phenotypically equivalent with identical NHR-6::GFP expression patterns, and were used for the ChIP-seq experiments.

### 2.2. Chromatin immunoprecipitation (ChIP)

Egg preparations were produced from ten large (100 mm) agar plates, containing growing cultures of either *nhr-6(lg6001); sgIs1* or *nhr-6 (lg6001); sgIs2* animals, by alkaline hypochlorite treatment [26]. Hatched, synchronized L1 arrested larvae from this procedure were then added to 20 large plates seeded with OP50 *E. coli* such that ~4,000 animals were placed on each plate. *nhr-6 (lg6001); sgIs1* animals were collected for the late L3/Early L4 and *nhr-6 (lg6001); sgIs2* animals were collected for the early-mid L4/mid L4 time points at 34-37 hours and 37-42 hours after plating respectively. A minimum of 20 animals were examined at high magnification (60x) with Nomarski optics to ensure they were at the correct developmental stage before proceeding. Crosslinking was then performed as previously described [27] to obtain multiple 1.5 mL Eppendorf tubes with 0.1 mL of packed animals each.

Fragmented chromatin was obtained by sonicating animal pellets on ice in 0.7 mL HLB buffer [28] using a Misonix Ultrasonic Liquid Sonicator S-4000 with the following settings: 50% amplitude, 5 second pulses with a 1 minute pulse-off period between each set of pulses. Each immunoprecipitation was performed using 2.2 mg of protein equivalent in the lysate as previously described [28] with either rabbit anti-eGFP IgG fraction (ThermoFisher #CAB4211) or control normal rabbit IgG (ThermoFisher #10500C)) antibodies. 50 $\mu$L of total lysate was used as non-treated input control. Purified DNA from each immunoprecipitation was run on a 1% agarose gel with ethidium bromide staining, and fragments of length 100-300 bp were excised and gel purified using the Omega Gel Extraction Kit (Omega BioTek) as per the manufacturer's protocol. Immunoprecipitated DNA samples along with purified input DNA for each developmental time point were sent to the Genomics Core Facility at Louisiana State University Pennington Biomedical Research Center for quality control analysis and next-generation sequencing using the Life Technologies SOLiD 5500xl Genetic Analyzer. Raw and processed

data have been deposited into GEO and can be accessed here: https://www.ncbi.nlm.nih.gov/geo/query/acc.cgi?acc=GSE96908.

For Western analysis of transgenic and non-transgenic animals, chromatin was immunoprecipitated using the Pierce Co-Immunoprecipitation Kit, according to manufacturer's instructions. Immunoprecipitation was performed with covalently immobilized polyclonal antibody to eliminate antibody interference in subsequent Western analysis. Western blots were probed with a monoclonal anti-eGFP (MAB3580, Millipore Sigma).

## 2.3. Mapping, peak-calling, and identification of target genes

ChIP sequence fragments were mapped to the *C. elegans* genome (version ce6) with the Short Read Mapping Package (SHRiMP) [29] alignment tool using the R/Bioconductor package BSgenome.Celegans.UCSC.ce6 [30]. Peaks were called using Model-based analysis of ChIP-Seq (MACS) [31] with the band width set at 300 and a p-value cutoff of 1.00 e-05 to generate a list of statistically significant enriched sequences through comparison to input sequences using default parameters. Enriched ChIP peaks were annotated with the R/Bioconductor package ChIPseeker [32] using the annotation package TxDB.Celegans.UCSC.ce6.ensGene [33].

## 2.4. Quantitative PCR

qPCR was performed using the BioRad CFX96 Real-time system and C1000 thermal cycler. All primers were designed using Primer3 [34] to ensure products of ~150 bp for each primer pair. The SsoFast$^{TM}$ EvaGreen Supermix (Bio-Rad) was utilized for SYBR Green quantification. Each reaction was set up in triplicate for DNA immunoprecipitated with the anti-eGFP antibody, DNA immunoprecipitated with the non-specific IgG antibody, and non-immunoprecipitated input DNA. The average Ct value for three technical repeats was generated and used to calculate $\Delta$Ct [(Ct value (sample) − Ct value (input)] and $\Delta\Delta$Ct values [$\Delta$Ct (experimental sample) − $\Delta$Ct (control)] [27]. Melt curve (disassociation plot) and efficiency ranges were used as quality control measures in each reaction. Fold enrichment between experimental sample and negative control was calculated using the formula $2^{(-\Delta\Delta Ct)}$.

## 2.5. RNAi screen

All RNAi experiments by feeding were performed on hatched L1 larvae [35] using a gene of interest RNAi plasmid-containing HT115 bacterial strain from the Open Biosystems RNAi library or the Source Bioscience RNAi library. Control RNAi experiments utilized HT115 bacteria transformed with a GFP RNAi plasmid (pPD128.110 (L447, Addgene)). Bacteria were freshly streaked out onto ampicillin (100 $\mu$g/mL)/tetracycline (12.5 $\mu$g/mL) plates and single colonies were cultured in 2 mL of LB broth in a 15 mL conical tube for 8 hours at 37° C with shaking. 75 $\mu$L of bacteria were spread onto NGM Lite plates containing 200 $\mu$g/mL ampicillin with 1 mM IPTG and induced overnight at 20° C. Synchronized L1 larvae from alkaline hypochlorite preparations were added to the freshly induced bacterial lawns and allowed to grow until the desired stage. When animals reached the adult stage they were screened for brood size abnormalities (decrease in number of eggs laid, abnormal egg morphology) for 48

hrs. RNAi experiments to quantify brood size and spermathecal morphology were performed as above with the following additions: ~50 animals were added to freshly-induced bacterial lawns and allowed to grow until young adult. Twenty animals for each strain were observed by Nomarski optics and scored for spermatheca cell number and morphology. Concurrently, fifteen animals from each experiment were moved to brood count plates and scored for brood size and abnormal egg morphology after 24 hours. Eggs were scored as abnormal when they displayed a small, roundish shape as previously described [19].

## 3. Results and Discussion

### 3.1. Identification of genome-wide NHR-6 binding sites

The spermatheca of adult *C. elegans* hermaphrodites consists of 24 cells that form a tube-like structure which serves as the site of sperm storage and oocyte fertilization [36]. Each adult animal consists of two spermathecae found on each side of the vulva that are characterized by a narrow distal constriction made up of eight cells while the remaining 16 cells form the wider bag-like chamber that connects to the proximal spermatheca-uterine valve. 18 of the 24 spermatheca cells are contributed from two large spermatheca precursor cells (SPCs) (9 from each) while the remaining six arise from the dorsal uterine (DU) lineage [37]. Each SPC cell is born in mid L3, the same time when NHR-6 expression is first observed in the spermatheca, and undergoes an asymmetric cell division just prior to entry into the fourth larval stage. Upon entry into L4, the larger of the two SPC daughter cells undergoes several rapid divisions while the smaller daughter cell divides once more to give the final total of 9 SPC daughter cells. Each of the six spermatheca cells contributed by the DU lineage arise very early in L4. High NHR-6 expression is observed in all cells that give rise to spermathecal cells beginning in the mid L3 stage and remains high in all 24 daughter cells until the mid L4 stage when it begins to diminish and is lost in the adult animal.

We have previously uncovered a critical role for *nhr-6* during this period of rapid SPC daughter cell divisions as these cells in *nhr-6*(*lg6001*) loss-of-function mutant animals fail to enter S-phase and undergo the correct number of divisions, resulting in an adult spermatheca with ~1/2 the number of normal cells [20]. Additionally, *nhr-6*(*lg6001*) mutants lack a spermatheca-uterine valve due to differentiation defects in the sujc cells that form the core of the valve [19]. When the cell number phenotype of *nhr-6*(*lg6001*) animals is suppressed to or near wild type numbers by loss of function of two different negative G1/S regulators [20], the spermatheca still fails to differentiate properly, indicating a dualistic role for *nhr-6* in both cell proliferation and cell differentiation. This work provided a detailed understanding of the timing of both spermatheca cell divisions and spermatheca cell differentiation and established an excellent *in vivo* model to study NR4A functions during these developmental processes.

To identify NR4A transcriptional programs that regulate spermatheca organogensis, we performed independent ChIP-seq experiments during both the late L3/early L4 and mid L4 time points. During this time, NHR-6 is robustly expressed in spermatheca cells (Figure 1A) which are undergoing several rapid divisions followed by differentiation respectively (Figure 1B). ChIP-seq was performed using an anti-eGFP antibody on animals carrying a functional full-length GFP tagged NHR-6 transgene (Figure 1C).

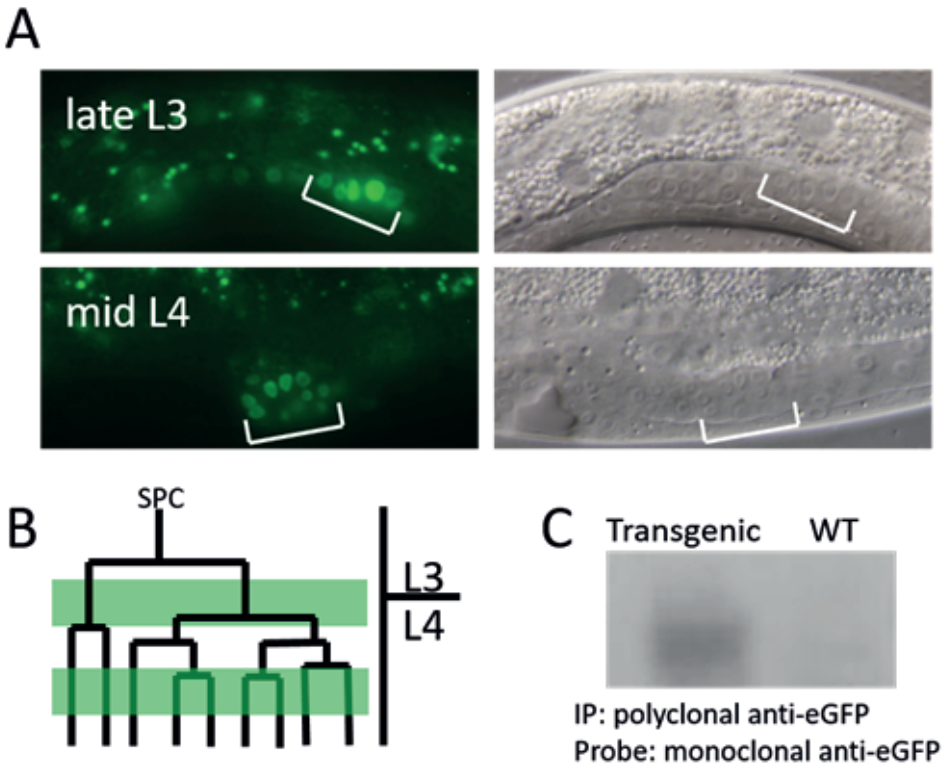


**Figure** 1: NHR-6::eGFP ChIP. **A.** Fluorescent and DIC images of NHR-6::eGFP localization in the spermathecae of late L3 (*sgIs1*) and mid L4 animals (*sgIs2*). White brackets indicate location of spermatheca cells. The surrounding punctate signal is gut autofluorescence, not GFP. **B.** Spermatheca precursor cell (SPC) lineage during L3 and L4. Green bars indicate time points at which animals were fixed for ChIP. **C.** Immunoblot of eGFP immunoprecipated from mixed stage *sgIs1* (Transgenic) and wildtype (WT) animals with immobilized polyclonal antibody.

Immunoprecipitated DNA fragments for each developmental stage along with non-treated control (Input) DNA were sequenced and sequencing tags were mapped to the *C. elegans* genome. Peaks were then called as enriched compared to input for each stage and were found to be evenly distributed across all chromosomes with a total of 5,071 binding sites found specifically in late L3/early L4; 4,457 specifically in mid L4; and 21,127 sites were found in both data sets (co-located) (Table 1). As described in detail previously [20, 21], NHR-6::GFP is also expressed at weaker levels in uterine and sheath cell precursor cells as cell divisions occur in the spermathecal lineage. Additionally, NHR-6::GFP is also expressed in two chemosensory neurons throughout larval development. Thus, binding sites identified from the ChIP-seq analysis would potentially also include NHR-6 binding sites from these cell types in addition to NHR-6 binding sites in spermathecal cells.

In order to immediately asses the reliability of the ChIP-seq data sets, 87 enriched binding sites that were found in both data sets were selected at random for quantitative PCR (qPCR) verification of enrichment. Cycle threshold (Ct) values were calculated for DNA sequences extracted with anti-eGFP and DNA extracted with non-specific anti-IgG antibodies. Fourteen sites were omitted due to poor qPCR quality leaving 73 total test sites. Sixty-five (89%) of these sites were verified as enriched with an average fold enrichment increase of 3.02 (data not shown).

**Table** 1: Distribution of NHR-6 binding sites compared across each chromosome.

| | late L3/early L4 | mid L4 | co-located | Total |
|---|---|---|---|---|
| **ChrI** | 905 | 904 | 4455 | 6264 |
| **ChrII** | 778 | 743 | 3612 | 5133 |
| **ChrIII** | 898 | 800 | 2990 | 4688 |
| **ChrIV** | 954 | 777 | 3523 | 5254 |
| **ChrV** | 868 | 798 | 3833 | 5499 |
| **ChrX** | 668 | 525 | 2714 | 3907 |
| **Total** | 5071 | 4547 | 21127 | 30745 |

## 3.2. Identification of candidate NHR-6 target genes

All enriched binding site coordinates for each stage were then annotated to determine their locations in relation to gene regulatory regions (Figure 2A and S1). Though *C. elegans* genes have been shown to have some distant (>2kb) control regions, it is typically found that the minimal promoter required for expression of RNA polymerase II transcripts is found within ∼2 kb upstream of the TSS and that this distance works well as a starting point when looking for cis-acting control elements [38]. Large introns may also contain additional regulatory elements. While most *C. elegans* introns are small (<100 bp), it has been shown that larger introns at the beginning of a coding region often contain regulatory elements [39, 40]. The majority of NHR-6 binding sites were found within 3 kb upstream (−3 kb) or 3 kb downstream (+3 kb) of a gene TSS when compared to the location of input peaks (Figure 2B). Therefore, we comprised a list of all genes for which an NHR-6 binding site was found either −3 kb or +3 kb of the TSS to represent a putative NHR-6 gene regulatory network.

Protein encoding genes were of particular interest for our functional analysis, and therefore, all genes encoding a small non-coding RNA or pseudogene were omitted. Additionally, we also filtered out sites within High Occupancy Target (HOT) regions that correspond to loci where multiple transcription factors have been shown to bind [2]. This comprehensive list was made to capture all or most candidate protein encoding target genes that have an NHR-6 binding site either in an upstream promoter region, possibly in a large first intron, or upstream of a possible transcript variant. These genes can be grouped depending on whether the binding sites associated with a gene is L3 specific (encompassing late L3/early L4 stages), L4 specific (mid-L4 stage), or co-located in both sets. There are seven possible groupings of these genes. There are 861 distinct genes associated only with L3 specific binding sites (L3 specific genes) and 729 distinct genes associated with L4 specific binding sites (L4 specific genes). The majority of genes only have co-located binding sites (4,153 genes) while the remaining have L3 specific and co-located binding sites (2,230 genes), L4 specific and co-located binding sites (1,723 genes), L3 specific and L4 specific binding sites (182 genes), and L3 specific, L4 specific, and co-located binding sites (1,977 genes). In total there are 13,126 distinct genes with TSSs found +/ − 3 kb of the binding site (S2). Among all peaks from both data sets, ∼70% can be found within −3 kb upstream of a gene TSS indicating NHR-6 primarily binds in the upstream regulatory regions of genes.

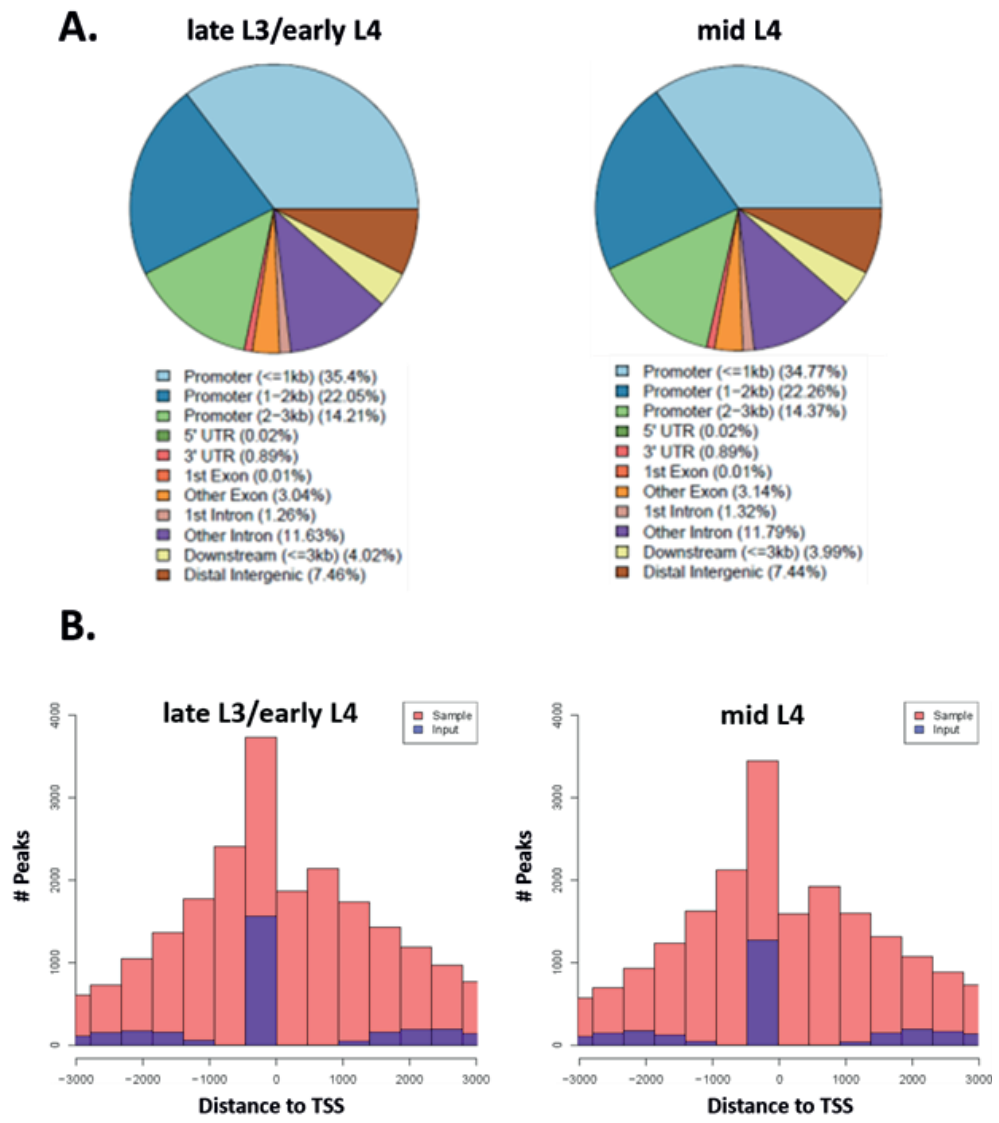


**Figure** 2: Genomic location of ChIP-seq peaks. **A.** Pie chart indicating the location of ChIP-seq peaks relative to gene locations. **B.** Total number and location of ChIP-seq peaks in relation to gene transcription start sites (TSS).

## 3.3. Pathway enrichment and gene ontology analysis of candidate NHR-6 target genes

In order to determine the cellular functions of NHR-6 candidate target genes, we examined them for enriched pathways and gene ontology terms. Analysis of enriched pathways was done for all protein encoding genes associated with stage-specific or co-located peaks using the R package PGSEA [41]. A total of 12 pathways in late L3/early L4, 4 in mid L4, and 52 in co-located data sets were found to be enriched (Figure 3). Most of the enriched pathways are involved in a variety of metabolic processes which would be active in rapidly proliferating cells and are known to be regulated by NR4A NR's [42, 43]. Additionally, quite a few signaling pathways were also enriched including the ErbB, MAPK, NOTCH, mTOR, Wnt , and Jak-STAT pathways. These pathways are involved in several critical processes including the propagation of growth signals


**Figure** 3: Heat map indicating enriched pathway scores of candidate NHR-6 target genes.

to facilitate cell cycle progression and proliferation as well as cell differentiation processes [44–49].

Gene ontology analysis for protein encoding genes using the DAVID bioinformatics resource (version 6.8) [50] uncovered several enriched biological process terms for candidate target genes in each stage (S3). Interestingly, genes involved in lipid storage, which is known to be regulated by NR4A NR's [3], were enriched in the co-located data set while regulation of Rho signaling, which is well studied for its role in *C. elegans* cellular morphogenesis [51–53], was enriched for candidate target genes in the mid L4 data set. Candidate target genes found in the co-located set

are involved in multiple cellular processes that are occurring in the spermatheca during these stages including the regulation of cell proliferation and spermatogenesis. It is worth noting that neuron fate commitment and specification were enriched in the co-located gene set. This is likely due to the fact that NHR-6 expression has been reported in some chemosensory neurons [18, 19], and mammalian NR4A NR's have been shown to regulate dopaminergic neuron development [54, 55]. Taken together, these results outline a putative NHR-6 regulatory network for further study of genes involved in cellular processes known to be regulated by NR4A NR's and known to be occurring in the spermatheca during these developmental stages. Additionally, the assortment of enriched processes and pathways these candidate target genes are involved in is congruent with much of the work done in mammalian systems, whereby the pleiotropic nature of NR4A receptors allows them to rapidly interconnect multiple signals into varied cellular responses.

## 3.4. qPCR validation of candidate NHR-6 target genes

We have extensively studied the spermatheca phenotypes of *nhr-6*(*lg6001*) null mutants as well as the division pattern of spermatheca cells in both wild type and mutant animals. Therefore, we used this information to manually select for a small subset of protein encoding NHR-6 candidate target genes that were likely, based on cellular function, to be involved in spermatheca development. Genes were analyzed with information found on wormbase.org as well as the gene ontology term with which they were described. All genes that did not fit into a gene ontology category and/or did not have any functional information on wormbase.org were omitted. We selected for genes that met some or all of the following criteria: have experimentally been shown to be involved in cell cycle regulation/division, cell differentiation, chromatin modification, cell signaling, or gene regulation, as well as any genes that are expressed in the spermatheca during L3 and L4. Using these criteria, we selected a total of 67 candidate target genes to validate for functions in spermatheca development as well as validate the associated binding sites through qPCR.

Separate ChIP experiments were performed to attain DNA used in each qPCR reaction, and primers were designed to ensure an amplicon size of ~150 bp for each pair. Of the 67 genes selected, we were unable to design usable primers for 13 of the associated binding sites and one site was upstream of multiple genes; therefore, a total of 53 binding sites were validated using qPCR. DNA immunoprecipated with anti-eGFP antibodies showed at least some enrichment over non-specific IgG DNA for each binding site using the ΔΔCt method of calculating fold enrichment while 27 (~51%) showed at least two fold enrichment (Table 2). Eight of these genes are known to be expressed in the spermatheca (*cye-1, hmg-1.2, tsp-21, riok-1, paa-1, eat-16, uaf-2, bet-1*). The majority of binding sites that were enriched at least two fold are associated with candidate target genes which function in cell cycle regulation, various signaling pathways, and chromatin modification.

Interestingly, the binding site with the largest fold increase corresponds to a site in the promoter of the sole *C. elegans* cyclin E gene, *cye-1*, which consequently is also found in the modENCODE data set for L4 animals [2]. Cyclin E is a key positive regulator of G1/S cell cycle progression, for which we have previously shown a requirement of *nhr-6* [20]. NR4A NR's have also been shown to regulate cyclin family members in mammalian tissues. For example, NR4A1 and NR4A3 upregulate Cyclin E in islet $\beta$-cells [56], and NR4A3 upregulates Cyclin D during

**Table** 2: **Candidate target genes with associated binding sites that displayed fold enrichment (FE) values ≥2**.

| Stage | Gene | Sequence | ddCt | FE | Function |
|---|---|---|---|---|---|
| co-located | *cye-1* | C37A2.4 | 4.78 | 27.47 | Cell Cycle |
| co-located | | F20B6.1 | 3.84 | 14.32 | Signaling |
| co-located | | F29A7.6 | 3.58 | 11.96 | Cell Cycle |
| co-located | *hmg-1.2* | F47D12.4 | 3.39 | 10.48 | Chromatin Regulation |
| co-located | *hpl-2* | K01G5.2 | 3.28 | 9.71 | Chromatin Regulation |
| co-located | *rpa-2* | M04F3.1 | 3.14 | 8.82 | Cell Cycle |
| co-located | | ZC123.4 | 2.92 | 7.57 | Cell Cycle |
| co-located | *zer-1* | T24C4.6 | 2.63 | 6.19 | Cell Cycle |
| co-located | *tsp-21* | C17G1.8 | 2.48 | 5.58 | Signaling |
| co-located | *jmjd-2* | Y48B6A.11 | 2.44 | 5.43 | Chromatin Regulation |
| co-located | *riok-1* | M01B12.5 | 2.39 | 5.24 | Signaling |
| co-located | *gei-1* | F45H7.2 | 2.2 | 4.59 | Signaling |
| co-located | *zfp-1* | F54F2.2 | 2.19 | 4.56 | Chromatin Regulation |
| mid L4 | | Y53F4B.3 | 2.09 | 4.26 | Cell Division |
| late L3/ mid L4 | *ntl-3* | Y56A3A.1 | 2.09 | 4.26 | Gene Regulation |
| co-located | *paa-1* | F48E8.5 | 2.03 | 4.08 | Signaling |
| co-located | *sipa-1* | T27F2.2 | 1.62 | 3.07 | Signaling |
| co-located | *swan-1* | F53C11.8 | 1.59 | 3.01 | Signaling |
| co-located | *nck-1* | ZK470.5 | 1.53 | 2.89 | Signaling |
| co-located | *eat-16* | C16C2.2 | 1.49 | 2.81 | Signaling |
| co-located | *sel-7* | K04G11.2 | 1.46 | 2.75 | Signaling |
| late L3/ mid L4 | *snr-4* | C52E4.3 | 1.41 | 2.66 | Splicing |
| co-located | *bet-2* | F57C7.1 | 1.39 | 2.62 | Chromatin Regulation |
| co-located | *dcp-66* | C26C6.5 | 1.36 | 2.57 | Chromatin Regulation |
| co-located | *uaf-2* | Y116A8C.35 | 1.3 | 2.46 | Splicing |
| mid L4 | *gex-3* | F28D1.10 | 1.26 | 2.39 | Signaling |
| co-located | *bet-1* | Y119C1B.8 | 1.23 | 2.34 | Chromatin Regulation |

smooth muscle cell proliferation [57]. Additionally, this binding site contains a canonical NBRE sequence which strongly suggest NHR-6 regulation of the *cye-1* gene. It should be noted that while this and some additional sites contained canonical NBRE sequences, or a variant of the NBRE sequence, a MEME analysis of all binding sites did not reveal the NBRE sequence as an overrepresented motif (data not shown); however, further analysis, including determining both monomer and hetero-/homodimer sites, is required to conclude if any one variant is enriched and represents an NHR-6 binding motif.

## 3.5. RNAi screen of selected candidate NHR-6 target genes

*nhr-6* RNAi has been shown to be hypomorphic in a wild-type N2 background [18]. However, *nhr-6* RNAi phenotypes in the RNAi sensitized *eri-1* mutant background are very similar with respect to spermatheca cell number and morphology to *nhr-6*(*lg6001*) mutant animals [18]. Additionally, *nhr-6* hypomorphic RNAi is strongly enhanced in *vab-2* and *jun-1* mutant backgrounds and NHR-6 has also been shown to interact with the JUN-1 transcription factor in a yeast two-hybrid assay [25]. A decrease in the amount of eggs laid and the presence of eggs laid with abnormal morphology is indicative of abnormal somatic gonad development and defective ovulation. Both of these phenotypes are observed in *nhr-6* mutant animals and are a direct result of abnormal spermatheca development. Therefore, these four mutant strains were used in an RNAi screen of the 67 candidate target genes previously selected to determine those that displayed reproductive phenotypes similar to *nhr-6*(*lg6001*) mutants. It was predicted that a gene with a critical role in spermatheca development would display a reproductive phenotype in either the wild-type N2 or sensitized *eri-1* mutant backgrounds, while an observed phenotype in either *vab-2* or *jun-1* mutant backgrounds would indicate a possible shared role in an *nhr-6* pathway, as well as provide a sensitized background to detect reproductive phenotypes. Thirteen of the 67 genes selected did not contain an RNAi clone in any RNAi library; therefore, a total of 54 genes were used for the screen.

An initial screen was performed that allowed young adult animals to lay eggs for 48 hours following RNAi by feeding, at which time plates were qualitatively screened for low brood sizes and/or an increase in abnormal egg morphology compared to control (GFP RNAi) animals. Of the 54 genes tested, 32 displayed a reproductive phenotype in at least one of the strains used, while 22 genes did not display any reproductive phenotypes (data not shown). We further analyzed the 32 genes which scored positive for reproductive defects by performing a detailed brood count analysis 24 hours after the animals reached the young adult stage. A total of 15 animals for each gene in each genetic background were scored. Eleven of the genes displayed a significant decrease in the average number of eggs laid with some also displaying abnormal egg morphology (Table 3). The majority of these genes contained corresponding NHR-6 binding sites found in the co-located data set while only one was found in each of the late L3/early L4 and mid L4 specific data sets. Interestingly, some of the selected genes showed strong reproductive phenotypes in one or more strains that were suppressed in a different genetic background. The high mobility group box gene *hmg-1.2*, the SWI/SNF complex component *let-526*, and *gei-1* which encodes a RhoGAP protein all displayed a strong phenotype in *eri-1* and *jun-1* mutant backgrounds that was suppressed in the *vab-2* mutant background, while the wingled-helix like transcription factor *lin-31* showed a strong reproductive phenotype in the *jun-1* mutant background that was suppressed in the other strains (Table 3).

In order to determine the specific cause of the reproductive defects, we analyzed animals from the 11 genes with significant brood count defects by DIC microscopy for spermatheca cell number and morphology defects similar to *nhr-6(lg6001)* mutants. Every gene scored showed abnormal spermatheca morphology in at least one genetic background compared to wild-type (Figure 4A), most notably a loss of distal constriction and failure of the SP-UT valve to form correctly. These phenotypes are readily detectable and were similar to those observed in *nhr-6*(*lg6001*) mutant animals (Figure 4B). The image in Figure 4C shows a representative example

**Table** 3: Average brood size following RNAi of selected genes.

| Stage | Gene | N2 (WT) | eri-1(-) | jun-1 (-) | vab-2 (-) |
|---|---|---|---|---|---|
| | *GFP* | 51.3 ± 9.6 | 44.8± 4.4 | 37.5± 6.4 | 40.3± 5.7 |
| **co-located** | *hmg-1.2* | 47.6± 8.7 | 1.9± 0.6* | **0** | 34.4± 4.8* |
| **co-located** | *dcp-66* | 53.7± 8.4 | 8.3± 0.8** | **2.1± 0.9*** | **14.9± 1.1** |
| **co-located** | *puf-9* | 48.3± 9.1 | 37.8±3.9 | **9.7± 3.7*** | **21.7± 4.1*** |
| **co-located** | *pas-5* | 0 | 0 | 0 | 0 |
| **co-located** | *let-526* | 47.8± 5.6 | 0 | **0.7± 0.3** | 36.6± 2.2 |
| **co-located** | *hpl-2* | 51.3± 7.3 | 41.7± 6.1 | 38.1± 6.6 | 44.3± 3.6 |
| **co-located** | *sop-3* | 49.6± 8.4 | 44.6± 4.3 | 35.9± 5.2 | 39± 4.2 |
| **co-located** | *sor-1* | 0 | 0 | 0 | 0 |
| **co-located** | *bet-1* | 44.3± 6.6 | 2.6± 1.3*** | **4.6± 1.5**** | **13± 2.8*** |
| **co-located** | *gei-1* | 49.9± 11.3 | 0.7± 0.3 | **14.3± 3.5**** | 38.9± 5.1 |
| **co-located** | *gei-13* | 5.4± 1.2* | 0.7± 0.5 | 6.1± 1.6 | 19.3± 3.2 |
| **late L3/early L4** | *gex-3* | 52.6±7.8 | 10.9±2.3** | **13±2.1** | **17.8± 2.9**** |
| **mid L4** | *lin-31* | 55.9± 5.3 | 38.6± 3.6 | **10.6±1.3**** | 39.3±3.7 |

Average brood size ± SD. N = 15 for each experiment. * = presence of abnormal eggs at ≥ 10% average; ** = presence of abnormal eggs at ≥ 25% average; *** = presence of abnormal eggs at ≥ 50% average. Bolded data indicate synergistic enhancement of brood size phenotype in *jun-1* and *vab-2* mutants compared to N2.

of the typical phenotypes observed; in the *eri-1*; *dcp-66*(RNAi) example there is clear loss of the distal constriction and SP-UT valve as well as overall loss of integrity of the organ. None of the selected genes scored displayed an abnormal spermatheca cell number phenotype. However, *let-526* RNAi did show a likely spermatheca cell number phenotype. An accurate quantification of the cell number phenotype of *let-526* could not be determined due to other abnormalities in the somatic gonad and germline that obscured spermatheca morphology. Nevertheless, a small number of animals could be observed that showed a marked decrease in cell number; a representative example of the phenotype observed is shown in Figure 4D.

The presence of an NHR-6 binding site in a regulatory region coupled with observed spermatheca phenotypes similar to *nhr-6*(*lg6001*) following RNAi of these genes suggests regulation by NHR-6 in a spermathecal development pathway. Further supporting a role for some these genes in a NHR-6 pathway is the genetic interactions observed in *jun-1* and *vab-2* mutants. It would be expected that at least some target genes of NHR-6 would exhibit genetic interactions similar to *nhr-6*. These genes, which were selected with a strong functional bias, represent only a very small number of probable NHR-6 target genes. Several selected genes that are likely to be involved in spermatheca development do not show any phenotypes following RNAi by feeding, which could be due to poor RNAi efficacy or redundancy, indicating that additional methods will need to be used to determine their role. RNA-seq studies on both wild-type and *nhr-6* loss of function animals will be necessary to confirm which genes associated with NHR-6 binding sites are either positively or negatively regulated by NHR-6. Nevertheless, these findings validate our selection method and outline an initial regulatory network whereby NHR-6 regulates cell cycle processes during the rapid proliferation stage of late L3 and early L4, and

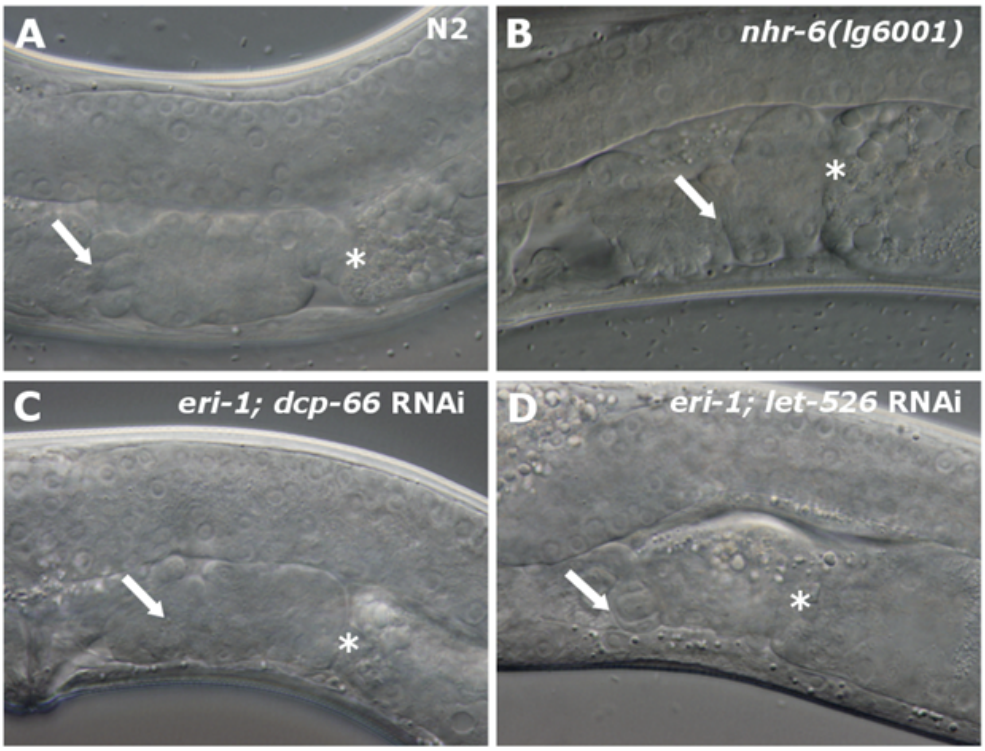


**Figure** 4: Spermatheca RNAi Phenotypes of NHR-6 Target Genes. **A.** Spermatheca of young adult N2 (WT) spermathecal. The spermathecal-uterine valve is indicated by the arrow, and the distal constriction is indicated by an asterisk. **B.** Young adult *nhr-6(lg6001)* mutant showing absence of both the spermathecal-uterine valve and the distal constriction. **C.** Spermatheca of young adult *dcp-66 (RNAi)* animal shows loss of normal morphology of the spermathecal-uterine valve and distal constriction, but spermathecal size (and cell number) is normal. This is the typical spermathecal morphology observed in animals displaying reproductive phenotypes in at least one of the mutant backgrounds. **D.** Spermatheca of young adult *let-526 (RNAi)* animal shows loss of normal morphology and a decreased organ size that is likely due to decreased cell number.

interconnects signals from multiple signaling pathways during mid L4 to ensure correct cell fate during morphogenesis of the spermatheca organ.

## Acknowledgements

We thank Phillip C.S.R. Kilgore, Urska Cvek, Marjan Trutschl, and Nayong Kim of the Louisiana Biomedical Research Network for helpful discussions of the data, and Hannah Knies for providing comments on the manuscript. Some nematode strains were obtained from the *Caenorhabditis* Genetics Center. This work was supported by a grant from the National Institute of General Medical Sciences (P20GM103424).

## Competing Interests

The authors declare no competing interests.

## References


[1] M. B. Gerstein, A. Kundaje, M. Hariharan et al., "Architecture of the human regulatory network derived from ENCODE data," *Nature*, vol. 489, no. 7414, pp. 91–100, 2012.

[2] M. B. Gerstein, Z. J. Lu, E. L. Van Nostrand, B. I. Arshinoff, and T. Liu, "Integrative analysis of the Caenorhabditis elegans genome by the modENCODE project. Science," *Science*, vol. 330, pp. 1775–1787, 2010.

[3] . Maxwell, "The NR4A subgroup: immediate early response genes with pleiotropic physiological roles," *Nuclear Receptor Signaling*, vol. 4, 2006.

[4] Z. Wang, G. Benoit, J. Liu et al., "Structure and function of Nurr1 identifies a class of ligand-independent nuclear receptors," *Nature*, vol. 423, no. 6939, pp. 555–560, 2003.

[5] T. E. Wilson, T. J. Fahrner, M. Johnston, and J. Milbrandt, "Identification of the DNA binding site for NGFI-B by genetic selection in yeast," *Science*, vol. 252, no. 5010, pp. 1296–1300, 1991.

[6] M. Maira, C. Martens, A. Philips, and J. Drouin, "Heterodimerization between members of the Nur subfamily of orphan nuclear receptors as a novel mechanism for gene activation," *Molecular and Cellular Biology*, vol. 19, no. 11, pp. 7549–7557, 1999.

[7] J. Martínez-González and L. Badimon, "The NR4A subfamily of nuclear receptors: New early genes regulated by growth factors in vascular cells," *Cardiovascular Research*, vol. 65, no. 3, pp. 609–618, 2005.

[8] T. Sekiya, I. Kashiwagi, R. Yoshida et al., "Nr4a receptors are essential for thymic regulatory T cell development and immune homeostasis," *Nature Immunology*, vol. 14, no. 3, pp. 230–237, 2013.

[9] R. N. Hanna, L. M. Carlin, H. G. Hubbeling et al., "The transcription factor NR4A1 (Nur77) controls bone marrow differentiation and the survival of Ly6C- monocytes," *Nature Immunology*, vol. 12, no. 8, pp. 778–785, 2011.

[10] S. P. Boudreaux, A. M. Ramirez-Herrick, R. P. Duren, and O. M. Conneely, "Genome-wide profiling reveals transcriptional repression of MYC as a core component of NR4A tumor suppression in acute myeloid leukemia," *Oncogenesis*, vol. 1, no. 7, article no. e19, 2012.

[11] H. N. Nowyhed, T. R. Huynh, A. Blatchley, R. Wu, G. D. Thomas, and C. C. Hedrick, "The Nuclear Receptor Nr4a1 Controls CD8 T Cell Development Through Transcriptional Suppression of Runx3," *Scientific Reports*, vol. 5, article no. 9059, 2015.

[12] J.-Y. Kim, H. C. Koh, J.-Y. Lee et al., "Dopaminergic neuronal differentiation from rat embryonic neural precursors by Nurr1 overexpression," *Journal of Neurochemistry*, vol. 85, no. 6, pp. 1443–1454, 2003.

[13] S. Hong, S. Chung, K. Leung, I. Hwang, J. Moon, and K.-S. Kim, "Functional roles of Nurr1, Pitx3, and Lmx1a in neurogenesis and phenotype specification of dopamine neurons during in vitro differentiation of embryonic stem cells," *Stem Cells and Development*, vol. 23, no. 5, pp. 477–487, 2014.

[14] F. Gizard, Y. Zhao, H. M. Findeisen et al., "Transcriptional regulation of S phase kinase-associated protein 2 by NR4A orphan nuclear receptor NOR1 in vascular smooth muscle cells," *Journal of Biological Chemistry*, vol. 286, no. 41, pp. 35485–35493, 2011.

[15] M. Vacca, S. Murzilli, L. Salvatore et al., "Neuron-derived orphan receptor 1 promotes proliferation of quiescent hepatocytes," *Gastroenterology*, vol. 144, no. 7, pp. 1518–e3, 2013.

[16] M. W. Maijenburg, C. Gilissen, S. M. Melief et al., "Nuclear receptors Nur77 and Nurr1 modulate mesenchymal stromal cell migration," *Stem Cells and Development*, vol. 21, no. 2, pp. 228–238, 2012.

[17] Z. Kostrouch, M. Kostrouchova, and J. E. Rall, "Steroid/thyroid hormone receptor genes in Caenorhabditis elegans," *Proceedings of the National Academy of Sciences of the United States of America*, vol. 92, no. 1, pp. 156–159, 1995.

[18] C. R. Gissendanner, K. Crossgrove, K. A. Kraus, C. V. Maina, and A. E. Sluder, "Expression and function of conserved nuclear receptor genes in Caenorhabditis elegans," *Developmental Biology*, vol. 266, no. 2, pp. 399–416, 2004.

[19] C. R. Gissendanner, K. Kelley, T. Q. Nguyen, M. C. Hoener, A. E. Sluder, and C. V. Maina, "The Caenorhabditis elegans NR4A nuclear receptor is required for spermatheca morphogenesis," *Developmental Biology*, vol. 313, no. 2, pp. 767–786, 2008.

[20] B. Praslicka and C. R. Gissendanner, "The C. elegans NR4A nuclear receptor gene nhr-6 promotes cell cycle progression in the spermatheca lineage," *Developmental Dynamics*, vol. 244, no. 3, pp. 417–430, 2015.

[21] M. Heard, C. V. Maina, B. E. Morehead et al., "A functional NR4A nuclear receptor DNA-binding domain is required for organ development in caenorhabditis elegans," *Genesis*, vol. 48, no. 8, pp. 485–491, 2010.

[22] W. Niu, Z. J. Lu, M. Zhong et al., "Diverse transcription factor binding features revealed by genome-wide ChIP-seq in C. elegans," *Genome Research*, vol. 21, no. 2, pp. 245–254, 2011.

[23] LD. Stein, Z. Bao, D. Blasiar, T. Blumenthal, MR. Brent, and N. Chen, *The genome sequence of Caenorhabditis briggsae: a platform for comparative genomics. PLoS biology*, 1(2, E45, 2003.

[24] S. Brenner, "The genetics of *Caenorhabditis elegans*," *Genetics*, vol. 77, no. 1, pp. 71–94, 1974.

[25] C. R. Gissendanner, D. Cardin, C. J. Dubose et al., "C. elegans nuclear receptor NHR-6 functionally interacts with the jun-1 transcription factor during spermatheca development," *Genesis*, vol. 52, no. 1, pp. 29–38, 2014.

[26] J. E. Sulston, "Neuronal cell lineages in the nematode Caenorhabditis elegans.," *Cold Spring Harbor Symposia on Quantitative Biology*, vol. 48, pp. 443–452, 1983.

[27] A. Mukhopadhyay, B. Deplancke, A. J. M. Walhout, and H. A. Tissenbaum, "Chromatin immunoprecipitation (ChIP) coupled to detection by quantitative real-time PCR to study transcription factor binding to DNA in Caenorhabditis elegans," *Nature Protocols*, vol. 3, no. 4, pp. 698–709, 2008.

[28] M. Zhong, W. Niu, Z. J. Lu et al., "Genome-wide identification of binding sites defines distinct functions for Caenorhabditis elegans PHA-4/FOXA in development and environmental response," *PLoS Genetics*, vol. 6, no. 2, Article ID e1000848, 2010.

[29] S. M. Rumble, P. Lacroute, A. V. Dalca, M. Fiume, A. Sidow, and M. Brudno, "SHRiMP: accurate mapping of short color-space reads," *PLoS Computational Biology*, vol. 5, no. 5, Article ID e1000386, 2009.

[30] Team TBD, BSgenome.Celegans.UCSC.ce6: Full genome sequences for Caenorhabditis elegans (UCSC version ce6). R package version 140. 2014.

[31] Y. Zhang, T. Liu, C. A. Meyer et al., "Model-based analysis of ChIP-Seq (MACS)," *Genome Biology*, vol. 9, no. 9, article R137, 2008.

[32] G. Yu, L.-G. Wang, and Q.-Y. He, "ChIP seeker: An R/Bioconductor package for ChIP peak annotation, comparison and visualization," *Bioinformatics*, vol. 31, no. 14, pp. 2382–2383, 2015.

[33] M. Carlson and BP. Maintainer, Maintainer BP. TxDb.Celegans.UCSC.ce6.ensGene: Annotation package for TxDb object(s). R package version 322. 2015.

[34] T. Koressaar and M. Remm, "Enhancements and modifications of primer design program Primer3," *Bioinformatics*, vol. 23, no. 10, pp. 1289–1291, 2007.

[35] L. Timmons, D. L. Court, and A. Fire, "Ingestion of bacterially expressed dsRNAs can produce specific and potent genetic interference in Caenorhabditis elegans," *Gene*, vol. 263, no. 1-2, pp. 103–112, 2001.

[36] J. McCarter, B. Bartlett, T. Dang, and T. Schedl, "Soma-germ cell interactions in Caenorhabditis elegans: Multiple events of hermaphrodite germline development require the somatic sheath and spermathecal lineages," *Developmental Biology*, vol. 181, no. 2, pp. 121–143, 1997.

[37] J. Kimble and D. Hirsh, "The postembryonic cell lineages of the hermaphrodite and male gonads in *Caenorhabditis elegans*," *Developmental Biology*, vol. 70, no. 2, pp. 396–417, 1979.

[38] V. Reinke, "Transcriptional regulation of gene expression in C. elegans," *WormBook*, pp. 1–31, 2013.

[39] P. G. Okkema, S. W. Harrison, V. Plunger, A. Aryana, and A. Fire, "Sequence requirements for myosin gene expression and regulation in Caenorhabditis elegans," *Genetics*, vol. 135, no. 2, pp. 385–404, 1993.

[40] S. Nam, Y.-H. Jin, Q.-L. Li et al., "Expression pattern, regulation, and biological role of Runt domain transcription factor, run, in Caenorhabditis elegans," *Molecular and Cellular Biology*, vol. 22, no. 2, pp. 547–554, 2002.

[41] K. A. Furge and Dykema K., Parametric Gene Set Enrichment Analysis. R package version 1480. 2012.

[42] Y. Zhao and D. Bruemmer, "NR4A orphan nuclear receptors: Transcriptional regulators of gene expression in metabolism and vascular biology," *Arteriosclerosis, Thrombosis, and Vascular Biology*, vol. 30, no. 8, pp. 1535–1541, 2010.

[43] H. S. Ranhotra, "The NR4A orphan nuclear receptors: Mediators in metabolism and diseases," *Journal of Receptors and Signal Transduction*, vol. 35, no. 2, pp. 184–188, 2015.

[44] D. C. Fingar, C. J. Richardson, A. R. Tee, L. Cheatham, C. Tsou, and J. Blenis, "mTOR controls cell cycle progression through its cell growth effectors S6K1 and 4E-BP1/eukaryotic translation initiation factor 4E," *Molecular and Cellular Biology*, vol. 24, no. 1, pp. 200–216, 2004.

[45] K. L. VanDussen, A. J. Carulli, T. M. Keeley et al., "Notch signaling modulates proliferation and differentiation of intestinal crypt base columnar stem cells," *Development*, vol. 139, no. 3, pp. 488–497, 2012.

[46] R. M. Weber-Nordt, R. Mertelsmann, and J. Finke, "The JAK-STAT pathway: Signal transduction involved in proliferation, differentiation and transformation," *Leukemia and Lymphoma*, vol. 28, no. 5-6, pp. 459–467, 1998.

[47] Y. Yarden and M. X. Sliwkowski, "Untangling the ErbB signalling network," *Nature Reviews Molecular Cell Biology*, vol. 2, no. 2, pp. 127–137, 2001.

[48] Z. Wei and H. T. Liu, "MAPK signal pathways in the regulation of cell proliferation in mammalian cells," *Cell Research*, vol. 12, no. 1, pp. 9–18, 2002.

[49] A.-M. Rajalin and P. Aarnisalo, "Cross-talk between NR4A orphan nuclear receptors and β-catenin signaling pathway in osteoblasts," *Archives of Biochemistry and Biophysics*, vol. 509, no. 1, pp. 44–51, 2011.

[50] D. W. Huang, B. T. Sherman, and R. A. Lempicki, "Systematic and integrative analysis of large gene lists using DAVID bioinformatics resources," *Nature Protocols*, vol. 4, no. 1, pp. 44–57, 2009.

[51] A. J. Piekny, A. Wissmann, and P. E. Mains, "Embryonic morphogenesis in Caenerhabditis elegans integrates the activity of LET-502 Rho-binding kinase, MEL-11 myosin phosphatase, DAF-2 insulin receptor and FEM-2 PP2c phosphatase," *Genetics*, vol. 156, no. 4, pp. 1671–1689, 2000.

[52] J. Gao, L. Estrada, S. Cho, R. E. Ellis, and J. L. Gorski, "Tha Caenorhabditis elegans homolog of FGD1, the human Cdc42 GEF gene responsible for faciogenital dysplasia, is critical for excretory cell morphogenesis," *Human Molecular Genetics*, vol. 10, no. 26, pp. 3049–3062, 2001.

[53] R. McMullan and S. J. Nurrish, "The RHO-1 RhoGTPase modulates fertility and multiple behaviors in adult C. elegans," *PLoS ONE*, vol. 6, no. 2, Article ID e17265, 2011.

[54] R. H. Zetterström, L. Solomin, L. Jansson, B. J. Hoffer, L. Olson, and T. Perlmann, "Dopamine neuron agenesis in Nurr1-deficient mice," *Science*, vol. 276, no. 5310, pp. 248–250, 1997.

[55] O. Saucedo-Cardenas, J. D. Quintana-Hau, W.-D. Le et al., "Nurr1 is essential for the induction of the dopaminergic phenotype and the survival of ventral mesencephalic late dopaminergic precursor neurons," *Proceedings of the National Academy of Sciences of the United States of America*, vol. 95, no. 7, pp. 4013–4018, 1998.

[56] J. S. Tessem, L. G. Moss, L. C. Chao et al., "Nkx6.1 regulates islet beta-cell proliferation via Nr4a1 and Nr4a3 nuclear receptors," *Proceedings of the National Academy of Sciences of the United States of America*, vol. 111, no. 14, pp. 5242–5247, 2014.

[57] T. Nomiyama, T. Nakamachi, F. Gizard et al., "The NR4A orphan nuclear receptor NOR1 is induced by platelet-derived growth factor and mediates vascular smooth muscle cell proliferation," *Journal of Biological Chemistry*, vol. 281, no. 44, pp. 33467–33476, 2006.